2-5 µm OBSERVATIONS OF EUROPA BY JUNO-JIRAM. G. Filacchione[1*], A. Adriani[1], A. Mura[1], F. Tosi[1], J. I. Lunine[2], A. Raponi[1], M. Ciarniello[1], D. Grassi[1], G. Piccioni[1], M. L. Moriconi[1], F. Altieri[1], C. Plainaki[3], G. Sindoni[3], R. Noschese[1], A. Cicchetti[1], S. J. Bolton[4], S. Brooks[5], [1]INAF-IAPS, Istituto di Astrofisica e Planetologia Spaziali, Area di Ricerca di Tor Vergata, via del Fosso del Cavaliere, 100, 00133, Rome, Italy, [2]Cornell University, Ithaca, NY, USA, [3]ASI, Agenzia Spaziale Italiana, via del Politecnico, snc, 00133, Rome, Italy, [4]Space Science and Engineering Division, Southwest Research Institute, San Antonio, TX, USA, [5]NASA-JPL, Pasadena, CA, USA, [*]corresponding author: gianrico.filacchione@inaf.it

Introduction: Between August 2016 and February 2018 JIRAM, the Jovian InfraRed Auroral Mapper [1], onboard the Juno mission has acquired four serendipitous observations of Europa. Due to Juno's high eccentricity polar orbits around Jupiter, the fixed orientation of the spacecraft spin axis and orbital plane placed along terminator, Europa is observed by JIRAM at approximately 90° phase angle from distances greater than 1.68E5 km resulting in a best spatial resolution of 42 km/px. The available dataset consists of about one thousand infrared spectra which cover a limited range in longitude but an almost complete excursion in latitude from poles to equator. We report about the spectral analysis of those data performed by applying several spectral indicators [2] suitable to characterize Europa surface composition, regolith grain size distribution and temperature.

JIRAM instrument shares a single telescope between an infrared imaging spectrometer and a dual-band camera [1]. The spectrometer (SPE) is characterized by a field of view (FOV) of 3.67° sampled by 256 spatial pixels and a spectral sampling of about 10 nm/band with 336 bands in the 2-5 µm range. The imager (IMG) relies on a push-frame design where a single array detector acquires images through two filters in band L (λ=3.455 µm, Δλ=0.29 µm) and M (λ=4.780 µm, Δλ=0.48 µm). These two spectral filters are optimized to observe Jupiter's auroras and thermal emission, respectively. Despite the Juno spacecraft being a spin axis-stabilized platform with an angular rotation rate of 2 r.p.m. specifically optimized to provide high-quality observations from Juno's particles and fields instruments, JIRAM is able to counter-compensate for this rotation by means of a motorized de-spinning mirror placed at the entrance of the telescope. To achieve this, the despinning mechanism axis is oriented parallel to the spacecraft rotation axis. The rotation of the mirror and the individual acquisitions of the SPE and IMG channels are commanded in time to allow capture of Europa when transiting through the instrumental FOV. Thanks to this solution it is possible to freeze the scene within the FOV for a maximum time of 1.2 sec during each 30 sec-long spacecraft rotation. During this period of time one hyperspectral slit in the 2-5 µm spectral range with the SPE channel and one image in band L and/or M with the IMG channel can be acquired. In Fig.1 is shown a typical average spectrum and L-M images of Europa by JIRAM. The instrumental SNR of the SPE channel is ≥100 in the 2-2.7 µm range, ≥ 30 in the 3-4.3 µm range and about 10 elsewhere.

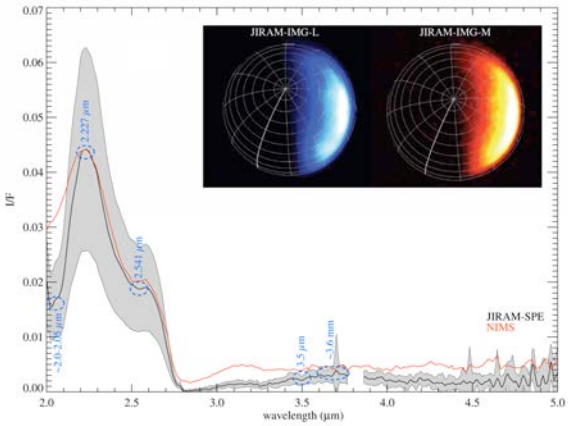

Figure 1. *Average I/F spectrum measured by the JIRAM-SPE channel on the dayside fraction of the Europa's northern pole region (black curve). The gray shadowed area shows the ±1 stdev computed on the 13 spectra used for the average. The dispersion corresponds to the changing illumination conditions and surface properties across Europa's disk. Wavelengths used to derive spectral indicators are labeled and discussed in the text. The weak feature of the hydrogen peroxide (H_2O_2) at 3.5 µm is indicated. An observation of Galileo/NIMS acquired on the Europa's northern polar region is shown for comparison (red curve, normalized to JIRAM at 2.227 µm; G. Hansen, personal communication). The inset panels contain polar projections of concurrent images acquired by the JIRAM IMG channel in band L (3.455 µm, left panel) and M (4.780 µm, right panel).*

Spectral Indicators: Since Europa's surface is dominated by water ice, a set of five spectral indicators is used to describe its physical state and composition. These indicators have been previously validated for the analysis of Saturn's icy satellites and rings data acquired by VIMS on Cassini [2,3]: 1) the 2 µm band center wavelength is used as a proxy of the water ice amorphous/crystalline state and of the non-ice material composition; 2) the 2 µm band depth is a proxy of wa-

ter ice and non-ice material abundance, regolith grain size distribution and solar phase. Since the JIRAM spectral range starts at 2.0 μm, it is not possible to resolve the short-wavelength wing of the water ice band but only its minimum. As a consequence, we compute the 2 μm band center and depth by fitting JIRAM data in the 2.0-2.2 μm with a 3rd-degree fit; 3) the ratio I/F(2.541 μm) / I/F(2.020 μm) is a proxy of the abundance of the non ice material; 4) the ratio I/F(3.630 μm) / I/F(2.227 μm) is a proxy of water ice grain size; 5) the wavelength of the I/F peak around 3.6 μm is a proxy of water ice temperature. The wavelengths corresponding to these indicators are marked in Fig. 1.

Results: on average the 2 μm water ice band center is observed at 2.038 μm as a result of the presence of both amorphous and crystalline ice phases and non-ice materials. The position of the band is shifting between 2.0 μm for amorphous ice and 2.05 μm for crystalline [4], with further dependence on temperature [5]. The reflectance intensity on the 2.4 μm inflection shoulder is comparable to the maximum absorption on the 2 μm band. A similar equalization of the ratio indicates the presence of non-ice materials, like magnesium chlorinated or hydrated magnesium salts [6], mixed with water ice. JIRAM data confirm the presence of a weak absorption band at 3.5 μm due to hydrogen peroxide (H_2O_2) first detected by Galileo/NIMS [7]. The surface regolith grain size is inferred by comparing the 2 μm band depth and the ratio I/F(3.63 μm) / I/F(2.27 μm) as in [2]. On the available dataset, average values of 0.6 for the first and 0.1 for the latter are measured, corresponding to water ice grain sizes encompassing the tens to hundreds of micron range. Despite the low signal-to-noise beyond 2.7 μm, due to the intrinsic low-reflectance of Europa's surface and the high (90°) solar phase angle occurring during the observations, JIRAM is able to measure the wavelength of the reflectance peak around 3.6 μm, which is a proxy of the temperature of water ice grains [8]. Our analysis shows that the peak's average wavelength occurs at 3.64 μm, corresponding to surface diurnal temperatures ≤131 K.

Discussion: spectral indicators evidence that the non-ice material is more abundant on the southern hemisphere relative to northern and in the Jupiter-facing hemisphere observed by JIRAM. A higher abundance of water ice (as inferred by means of the 2 μm band depth) is observed on the northern polar region. This result confirms the water ice enrichment seen on the north pole bright plains by Galileo/NIMS [9]. Moreover, JIRAM data indicate a typical regolith grain size distribution ranging between tens and hundreds of microns: this result is in agreement with independent analyses of Europa's infrared reflectance spectra [10,11,12] and polarimetric observations [13]. The presence of a second, less numerous population of larger (>100 μm) grains measured mainly on the northern hemisphere is evident from the analysis of spectral indicators. A similar grain size distribution makes the surface of Europa distinctively different with respect to other icy satellites, like those of Saturn, where small grains (<80 μm) dominate [2,14,15]. Several active processes might result in the coalescence of the grains up to mm-sizes on Europa: the resurfacing on the chaos terrains, the thermal sintering caused by the high Jovian temperatures and the bombardment by energetic particles. All these effects are more important in Jupiter's environment than at Saturn, where temperature and radiation effects are much lower. In addition, all of Saturn's icy satellites orbiting within the E-ring are weathered by the deposition of micron and submicron grains ejected from Enceladus' plumes [16] and mantling their surfaces. Finally, the presence of larger abundances of amorphous ice observed by JIRAM across the north-equatorial region can be explained with the bombardment of magnetospheric particles occurring preferentially in this region [17]. Further observations of Europa are currently planned by the JIRAM team before the end of the Juno mission, which will help us to improve our analyses.

Acknowledgments: The authors acknowledge the financial support from Italian Space Agency (ASI) for the Juno-JIRAM program through ASI-INAF agreement number 2016-23-H.0 and for the US authors, NASA. This research has made use of NASA's Astrophysics Data System. All data used in this work are publicly available through NASA-PDS.

References: [1] Adriani, A. et al. (2017) *SSR*, 213, 393-446. [2] Filacchione, G.. et al. (2012) *Icarus, 220, 1064-1096*. [3] Filacchione, G.. et al. (2014) Icarus, 241, 45-65. [4] Mastrapa, R. M. et al. (2008), Icarus, 197, 307-320. [5] Grundy W. M. and Schmitt, B. (1998) *JGR*, 103, E11, 25809-25822. [6] Hanley, J. et al. (2014), *JGR*, 109 (E1). [7] Carlson, R. W. et al. (1999) *Science,* 283, 2062. [8] Filacchione, G. et al. (2016) *Icarus*, 271, 292-313. [9] Fanale, F. P. et al. (1999), *Icarus*, 139, 179-188. [10] Hansen, G. B. and McCord, T., (2004), *JGR*, 109(E1). [11] Dalton, J. B. et al (2012), *JGR*, 117(E03003). [12] Ligier, N. et al. (2016), Astr. J., 151(6), 163. [13] Poch, O. et al., (2018), *JGR*, 123, 2564-2584. [14] Verbiscer, A. J., et al. (2006), *Icarus*, 182, 211-223. [15] Ciarniello, M., et al. (2011), *Icarus*, 214, 541-555. [16] Porco, C. C. et al. (2006), *Science*, 311, 1393-1401. [17] Nordheim, T. A. et al. (2018), *Nature Astronomy*, 2, 673-679.